Inorganic Chemistry

Article

pubs.acs.org/IC

Hydroflux Crystal Growth of Platinum Group Metal Hydroxides: $Sr_6NaPd_2(OH)_{17}$, $Li_2Pt(OH)_6$, $Na_2Pt(OH)_6$, $Sr_2Pt(OH)_8$, and $Ba_2Pt(OH)_8$

Daniel E. Bugaris, Mark D. Smith, and Hans-Conrad zur Loye*

Department of Chemistry and Biochemistry, University of South Carolina, Columbia, South Carolina 29202, United States

Supporting Information

ABSTRACT: Crystals of five complex metal hydroxides containing platinum group metals were grown by a novel low-temperature hydroflux technique, a hybrid approach between the aqueous hydrothermal and the molten hydroxide flux techniques. $Sr_6NaPd_2(OH)_{17}$ (**1**) crystallizes in orthorhombic space group *Pbcn* with lattice parameters a = 19.577(4) Å, b = 13.521(3) Å, and c = 6.885(1) Å. This compound has a three-dimensional framework structure with $Sr(OH)_n$ polyhedra, $Na(OH)_6$ octahedra, and $Pd(OH)_4$ square planes. Isostructural phases $Li_2Pt(OH)_6$ (**2**) and $Na_2Pt(OH)_6$ (**3**) crystallize in trigonal space group *P*-3 with lattice parameters of a = 5.3406(8) Å and c = 4.5684(9) Å and a = 5.7984(8) Å and c = 4.6755(9) Å, respectively. Structures of these materials consist of layers of $A(OH)_6$ (A = Li (**2**), Na (**3**)) and $Pt(OH)_6$ octahedra. $Sr_2Pt(OH)_8$ (**4**) crystallizes in monoclinic space group $P2_1/c$ with lattice parameters a = 5.9717(6) Å, b = 10.997(1) Å, c = 6.0158(6) Å, and β = 113.155(2)°, while $Ba_2Pt(OH)_8$ (**5**) crystallizes in orthorhombic space group *Pbca* with lattice parameters a = 8.574(2) Å, b = 8.673(2) Å, and c = 10.276(2) Å. Both of these compounds have three-dimensional structures composed of $Pt(OH)_6$ octahedra surrounded by either $Sr(OH)_8$ or $Ba(OH)_9$ polyhedra. Decomposition of these materials into condensed metal oxides, which is of importance to possible catalytic applications, was monitored via thermogravimetric analysis. For example, $Na_2Pt(OH)_6$ (**3**) converts cleanly via dehydration into α-Na_2PtO_3.

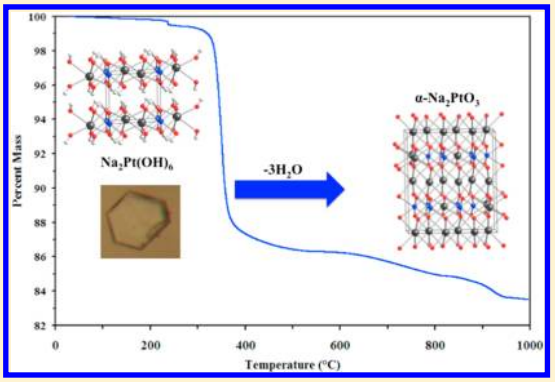

INTRODUCTION

There is renewed interest in and emphasis on crystal growth techniques in both the solid-state chemistry and the materials science communities. Ready access to high-quality single crystals allows for both accurate structure determination (by both X-ray and neutron diffraction methods) and physical property measurements. The ability to establish detailed structure−property relationships provides important data that can be used by theoretical scientists in their efforts to computationally address pressing issues in areas such as energy storage and transmission, catalysis, data storage (computing), etc.

Various crystal growth techniques have been applied to the synthesis of inorganic materials, with two of the most popular and effective being hydrothermal (supercritical water) methods and high-temperature solutions (fluxes).[1] Both of these techniques have been utilized extensively to prepare complex metal oxides.[2] Hydrothermal methods take advantage of the high pressures generated by supercritical water in closed vessels to aid in dissolution of starting materials and crystallization of the final products. High-temperature solutions employ a low-melting (in relative terms, less than 1000 °C) inorganic compound to act as a solvent for dissolution of reagents and nucleation/crystallization of the intended products. In particular, alkali metal hydroxides have proven to be excellent fluxes for growth of high-quality crystals of oxide materials.[3]

Recently, we explored a synthetic regime that operates at the interface of the hydrothermal and flux methods and is referred to as a low-temperature hydroflux. In this technique, the crystal growth reaction is operating in an aqueous solution of alkali metal hydroxides at temperatures where the water has not reached a critical state. Little or no pressure is generated at the maximum temperature during the reaction, so we are relying solely upon addition of water to further decrease the already low melting point of the alkali metal hydroxides.

One of the unique aspects of the hydroflux technique is that complex metal hydroxides can be grown as single crystals. In typical flux reactions with alkali metal hydroxides at higher temperatures, the product is typically an oxide, with only rare cases whereby a hydroxide (specifically an oxyhydroxide[4]) is formed. However, with the hydroflux technique, complex metal hydroxides can be rapidly and reliably synthesized in crystalline form. Complex metal hydroxides, or hydroxymetallates, are a relatively unexplored class of materials. Those hydroxymetallates that have appeared in the literature generally contain an electropositive alkali or alkaline earth metal along with a first-row transition metal or main group metal. In this paper, we extend the hydroflux method we previously introduced for the series $A_2M(OH)_6$ (A = Sr, Ba; M = Mn, Co, Ni, Cu)[5] to the

Received: November 13, 2012

   dx.doi.org/10.1021/ic302439b | Inorg. Chem. XXXX, XXX, XXX−XXX

Table 1. Structure Refinement Details from Single-Crystal X-ray Diffraction

empirical formula	$Sr_6NaPd_2(OH)_{17}$	$Li_2Pt(OH)_6$	$Na_2Pt(OH)_6$	$Sr_2Pt(OH)_8$	$Ba_2Pt(OH)_8$
temp, (K)	100	100	100	298	298
wavelength (Å)	0.71073	0.71073	0.71073	0.71073	0.71073
space group	*Pbcn*	*P*-3	*P*-3	$P2_1/c$	*Pbca*
Z	4	1	1	2	4
fw	1050.65	311.02	343.12	506.39	605.83
a (Å)	19.577(4)	5.3406(8)	5.7984(8)	5.9717(6)	8.574(2)
b (Å)	13.521(3)	5.3406(8)	5.7984(8)	10.997(1)	8.673(2)
c (Å)	6.885(1)	4.5684(9)	4.6755(9)	6.0158(6)	10.276(2)
β (deg)	90	90	90	113.155(2)	90
V (Å^3)	1822.5(6)	112.84(3)	136.14(4)	363.24(6)	764.1(3)
ρ_c (g cm^{-3})	3.829	4.577	4.185	4.630	5.266
μ (mm^{-1})	19.446	31.019	25.879	33.842	28.460
F(000)	1936	138	154	452	1048
cryst size (mm)	0.20 × 0.08 × 0.02	0.10 × 0.08 × 0.06	0.06 × 0.04 × 0.04	0.20 × 0.03 × 0.03	0.10 × 0.09 × 0.07
θ_{max} (deg)	28.28	38.48	28.29	28.32	28.26
no. of reflns collected	31 946	2989	1508	4860	9569
no. of independent reflns	2259	433	231	899	947
goodness-of-fit on F^2	1.022	1.090	1.152	1.198	1.314
min/max transmission	0.3524/0.7457	0.0322/0.0826	0.4836/0.7457	0.3325/0.7457	0.5380/0.7457
$R(F)$	0.0256	0.0144	0.0105	0.0164	0.0147
$R_w(F^2)$	0.0629	0.0345	0.0254	0.0412	0.0293
largest diff. peak/hole (e$^-$ Å^{-3})	1.098 and −0.938	2.939 and −2.578	0.888 and −0.998	1.255 and −2.219	0.776 and −1.203

platinum group metals for compounds $Sr_6NaPd_2(OH)_{17}$ (**1**), $Li_2Pt(OH)_6$ (**2**), $Na_2Pt(OH)_6$ (**3**), $Sr_2Pt(OH)_8$ (**4**), and $Ba_2Pt(OH)_8$ (**5**). Few platinum group metal containing hydroxides have been reported in the literature, though there are some examples for Pd[6−11] and Pt[12−20] as well as some oxyhydroxides for Re,[4] Ru,[21−23] Os,[24−33] and Pt.[16] It should be noted that a number of these compounds lack characterization beyond a single-crystal X-ray structure determination, if even that.

The value in synthesizing these complex metal hydroxides is 2-fold, with the first benefit being the chemical intuition to be gained from preparing and characterizing novel compositions. For example, recent computational work has pointed toward alkali metal-stabilized Pt hydroxo species as the active catalytic species in the Pt-catalyzed water−gas shift reaction.[34] A thorough investigation of our currently reported complex Pt hydroxide compounds may shed some experimental light in this area. The second and perhaps more practical value of synthesizing metal hydroxides is for their use as precursors to oxide materials. Gentle heating of metal hydroxides leads to dehydration and yields metal oxides at much lower temperatures than required in conventional solid-state reactions. A recent report detailed the cost-effective, low-temperature synthesis of $Na_xPt_3O_4$ (both a catalyst and an oxygen electrode material for alkaline fuel cells) in thin film form.[35] Dehydration of metal hydroxides may be an equally viable route to technologically important metal oxides. Therefore, we also discuss here the decomposition of our platinum group metal containing hydroxides as monitored by a combination of thermogravimetric analysis and powder X-ray diffraction.

EXPERIMENTAL METHODS

Reagents. The following reagents were used as obtained: $LiOH·H_2O$ (Alfa Aesar), NaOH (J. T. Baker), KOH (Fisher), $Sr(OH)_2·8H_2O$ (Alfa Aesar, 99%), $Ba(OH)_2·8H_2O$ (Alfa Aesar, 98%), and K_2PdCl_6 (Alfa Aesar). A 0.33 M solution of $H_2[PtCl_6]$ was prepared from Pt (Engelhard, 99.95%) by a literature procedure.[36]

Single-Crystal Growth. Single crystals of the reported materials were grown by hydroflux techniques. A 0.1312 g amount of K_2PdCl_6, 0.1759 g of $Sr(OH)_2·8H_2O$, 3.9 g of NaOH, and 5.5 g of KOH (5.5 g) for $Sr_6NaPd_2(OH)_{17}$ (**1**), 1 mL of $H_2[PtCl_6]$, 1.28 g of $LiOH·H_2O$, and 4 g KOH for $Li_2Pt(OH)_6$ (**2**), 1 mL of $H_2[PtCl_6]$ and 5 g NaOH for $Na_2Pt(OH)_6$ (**3**), 1 mL of $H_2[PtCl_6]$, 0.2657 g of $Sr(OH)_2·8H_2O$, and 5 g of NaOH for $Sr_2Pt(OH)_8$ (**4**), and 1 mL of $H_2[PtCl_6]$, 0.2082 g of $Ba(OH)_2·8H_2O$, 2.5 g of NaOH, and 2.5 g of KOH for $Ba_2Pt(OH)_8$ (**5**) were dissolved in 10 mL of deionized H_2O in 25 mL polytetrafluoroethylene (PTFE) lined stainless steel autoclaves. The autoclaves were placed in an oven and heated at either 0.5 (for $Sr_6NaPd_2(OH)_{17}$ (**1**) and $Na_2Pt(OH)_6$ (**3**)) or 1 °C/min (for the other three compounds) to 230 °C. Reactions were held at 230 °C for 24 h, followed by cooling at 0.1 (for $Sr_2Pt(OH)_8$ (**4**) and $Ba_2Pt(OH)_8$ (**5**)) or 0.3 °C/min (for the other three compounds) to room temperature. Single-crystal products form in essentially quantitative yield (based on the starting Pd or Pt precursor) and were isolated by vacuum filtration while rinsing with methanol. Morphologies and colors of the crystals were long orange plates for $Sr_6NaPd_2(OH)_{17}$ (**1**), pale yellow hexagonal prisms for $Li_2Pt(OH)_6$ (**2**) and $Na_2Pt(OH)_6$ (**3**), long pale yellow plates for $Sr_2Pt(OH)_8$ (**4**), and pale yellow octahedral prisms for $Ba_2Pt(OH)_8$ (**5**). In the reaction to form $Li_2Pt(OH)_6$ (**2**), colorless plate crystals (identified as a mixture of $LiOH·H_2O$ and Li_2CO_3 by powder X-ray diffraction) could be mechanically separated. In the reaction for $Ba_2Pt(OH)_8$ (**5**), colorless block crystals (identified as $BaCO_3$ by powder X-ray diffraction) were also found. No other single-crystalline materials were found in the remaining products.

Scanning Electron Microscopy. Single crystals of all five compounds were analyzed by scanning electron microscopy using an FEI Quanta SEM instrument utilized in low-vacuum mode. Energy-dispersive spectroscopy verified the presence of the appropriate alkali and/or alkaline earth metals, Pd or Pt, and O. Within the detection limits of the instrument (0.1 wt %), the absence of extraneous elements such as K or Cl was confirmed.

Single-Crystal X-ray Diffraction. Single-crystal X-ray diffraction data were collected with the use of graphite-monochromatized Mo Kα radiation (λ = 0.71073 Å) on a Bruker SMART APEX diffractometer. Data were collected at 100 K for $Sr_6NaPd_2(OH)_{17}$ (**1**), $Li_2Pt(OH)_6$ (**2**), and $Na_2Pt(OH)_6$ (**3**) and at 298 K for $Sr_2Pt(OH)_8$ (**4**) and $Ba_2Pt(OH)_8$ (**5**). For $Sr_2Pt(OH)_8$ (**4**) and $Ba_2Pt(OH)_8$ (**5**), data were collected by a scan of 0.3° in ω in groups of 606 frames at φ settings of

dx.doi.org/10.1021/ic302439b | Inorg. Chem. XXXX, XXX, XXX−XXX

0°, 90°, 180°, and 270° with an exposure time of 20 s/frame. For $Sr_6NaPd_2(OH)_{17}$ (**1**), $Li_2Pt(OH)_6$ (**2**), and $Na_2Pt(OH)_6$ (**3**), both ω and φ scans were collected with an exposure time of 15 s/frame. Collection of intensity data was carried out with the program SMART.[37] Cell refinement and data reduction were carried out with the program SAINT+.[37] Empirical absorption corrections were performed with the program SADABS.[37] Structures were solved with the direct methods program SHELXS and refined with the full-matrix least-squares program SHELXL.[38] After H atoms were located by difference Fourier syntheses, O−H bond lengths were restrained to d = 0.85(2) Å using the DFIX command. Final refinements included anisotropic displacement parameters for the metal and O atoms and isotropic displacement parameters for the H atoms. In all structures, restrained refinement of H-atom parameters resulted in physically reasonable displacement parameters (similar in magnitude to the parent O atoms) and no unacceptably short interatomic contact distances, providing strong support for the reported positions. A secondary extinction correction was included for compounds other than $Sr_6NaPd_2(OH)_{17}$ (**1**). Additional experimental details are given in Table 1 and the Supporting Information. Selected metrical details are presented in Tables 2−4.

Table 2. Selected Interatomic Distances (Angstroms) for $Sr_6NaPd_2(OH)_{17}$ (1)

Sr(1)−O(2)	2.470(3)	Sr(3)−O(5)	2.556(3)
Sr(1)−O(6)	2.565(3)	Sr(3)−O(8)	2.575(3)
Sr(1)−O(9)	2.627(3)	Sr(3)−O(5)	2.585(3)
Sr(1)−O(8)	2.628(3)	Sr(3)−O(4)	2.591(3)
Sr(1)−O(6)	2.640(3)	Sr(3)−O(3)	2.599(3)
Sr(1)−O(2)	2.678(3)	Sr(3)−O(4)	2.637(3)
Sr(1)−O(9)	2.7078(6)	Sr(3)−O(3)	2.711(3)
Sr(1)−O(4)	2.888(3)	Sr(3)−O(6)	2.934(3)
Sr(1)−O(2)	3.122(4)	Sr(3)−O(7)	2.963(3)
Sr(2)−O(7)	2.530(3)		
Sr(2)−O(1)	2.544(3)	Na−O(8) × 2	2.372(3)
Sr(2)−O(1)	2.548(3)	Na−O(2) × 2	2.387(3)
Sr(2)−O(1)	2.556(3)	Na−O(1) × 2	2.581(3)
Sr(2)−O(7)	2.582(3)		
Sr(2)−O(8)	2.617(3)	Pd−O(6)	2.015(3)
Sr(2)−O(3)	2.639(3)	Pd−O(4)	2.020(3)
		Pd−O(7)	2.027(3)
		Pd−O(3)	2.032(3)

Table 3. Selected Interatomic Distances (Angstroms) for $Li_2Pt(OH)_6$ (2) and $Na_2Pt(OH)_6$ (3)

	A = Li	A = Na
A−O × 3	2.036(4)	2.329(2)
A−O × 3	2.236(6)	2.428(2)
Pt−O × 6	2.006(2)	2.017(2)

Powder X-ray Diffraction. Powder X-ray diffraction data were collected on a Rigaku D/Max-2100 powder X-ray diffractometer using Cu Kα radiation. The step−scan covered the angular range 10−80° 2θ in steps of 0.02°.

Thermal Analyses. Thermogravimetric analyses were carried out on a TA Instruments SDT Q600 simultaneous DTA-TGA by heating the single crystals of both $Na_2Pt(OH)_6$ (**3**) and $Sr_2Pt(OH)_8$ (**4**) at a rate of 5 °C/min under flowing air up to a temperature of 1000 °C.

Infrared Spectroscopy. Infrared spectra of ground single crystals of the five title compounds were collected at room temperature on a Perkin-Elmer Spectrum 100 FT-IR spectrometer equipped with an ATR attachment in the range 650−4000 cm^{-1}. Previous reports in the literature have indicated δ(OH) deformation bands to be present in the region 600−1000 cm^{-1} and ν(OH) stretching bands to be present in the region 2600−3600 cm^{-1}.[9,11] Bands in these regions are observed in spectra of all five title compounds (Supporting Information).

Table 4. Selected Interatomic Distances (Angstroms) for $Sr_2Pt(OH)_8$ (4) and $Ba_2Pt(OH)_8$ (5)

$Sr_2Pt(OH)_8$		$Ba_2Pt(OH)_8$	
Sr−O(4)	2.488(3)	Ba−O(1)	2.692(3)
Sr−O(2)	2.566(3)	Ba−O(2)	2.723(3)
Sr−O(2)	2.572(3)	Ba−O(3)	2.753(3)
Sr−O(4)	2.650(3)	Ba−O(3)	2.759(3)
Sr−O(1)	2.668(3)	Ba−O(4)	2.791(3)
Sr−O(3)	2.669(3)	Ba−O(1)	2.910(3)
Sr−O(3)	2.689(3)	Ba−O(4)	2.934(3)
Sr−O(1)	2.747(3)	Ba−O(2)	3.019(3)
		Ba−O(2)	3.108(3)
Pt−O(3) × 2	2.014(3)		
Pt−O(2) × 2	2.014(3)	Pt−O(2) × 2	1.990(2)
Pt−O(1) × 2	2.018(3)	Pt−O(3) × 2	1.996(3)
		Pt−O(4) × 2	2.003(3)

RESULTS AND DISCUSSION

Syntheses. All reactions were performed in PTFE-lined stainless steel autoclaves at 230 °C. Reaction yields were essentially quantitative based on the amount of starting Pd or Pt precursor. $Sr_6NaPd_2(OH)_{17}$ (**1**) was synthesized from the Pd^{4+} precursor, K_2PdCl_6, in a hydroflux containing $Sr(OH)_2{\cdot}8H_2O$, NaOH, and KOH. Attempts to repeat the synthesis with a Pd^{2+} precursor, $Pd(NH_3)_2Cl_2$, instead yielded primarily Pd metal. This suggests that reduction of Pd is occurring in the hydroflux, from Pd^{4+} in K_2PdCl_6 to Pd^{2+} in $Sr_6NaPd_2(OH)_{17}$ (**1**), and from Pd^{2+} in $Pd(NH_3)_2Cl_2$ to Pd^0 in elemental Pd. Long thin orange plates, up to ∼2 mm in length, of $Sr_6NaPd_2(OH)_{17}$ (**1**) were obtained in this reaction.

For the Pt-containing reactions, both the Pt precursor, $H_2[PtCl_6]$, and the final products contained Pt^{4+}. In contrast to the reaction with Pd, no reduction of Pt occurred in any of the reactions. $Li_2Pt(OH)_6$ (**2**), $Na_2Pt(OH)_6$ (**3**), and $Ba_2Pt(OH)_8$ (**5**) all formed as prismatic crystals, whereas crystals of $Sr_2Pt(OH)_8$ (**4**) assumed a plate-like morphology. The largest crystals of each compound were several millileters in their longest dimension.

Structures. $Sr_6NaPd_2(OH)_{17}$ (**1**) crystallizes in a new structure type in space group *Pbcn* of the orthorhombic system (Figure 1). The asymmetric unit comprises 3 Sr atoms, 1 Na atom, 1 Pd atom, 9 O atoms, and 9 H atoms. Na and O(9) atoms have site symmetry .2., whereas all other atoms are on general positions. Na and Pd atoms are bonded to a distorted octahedron and a square plane of OH^- anions, respectively. Sr(1) and Sr(3) are each bonded to 9 OH^- anions, with a square face tricapped trigonal prismatic geometry. Sr(2) is coordinated with 7 OH^- anions in a distorted face-capped octahedron. On the basis of charge electroneutrality, the formal oxidation state of Pd can be assigned as +2.

The structure of $Sr_6NaPd_2(OH)_{17}$ (**1**) consists of a three-dimensional framework of the $Sr(OH)_n$ polyhedra with channels extending along the z axis (Figure 2). These channels are alternately occupied by the $Na(OH)_6$ octahedra and the $Pd(OH)_4$ square planes. In the framework, each Sr(1) polyhedron shares corners with one Sr(1) polyhedron, one Sr(2) polyhedron, and two Sr(3) polyhedra and shares faces with four Sr(1) polyhedra and one Sr(3) polyhedron. Every Sr(2) polyhedron corner shares with one Sr(1) polyhedra and

dx.doi.org/10.1021/ic302439b | Inorg. Chem. XXXX, XXX, XXX−XXX

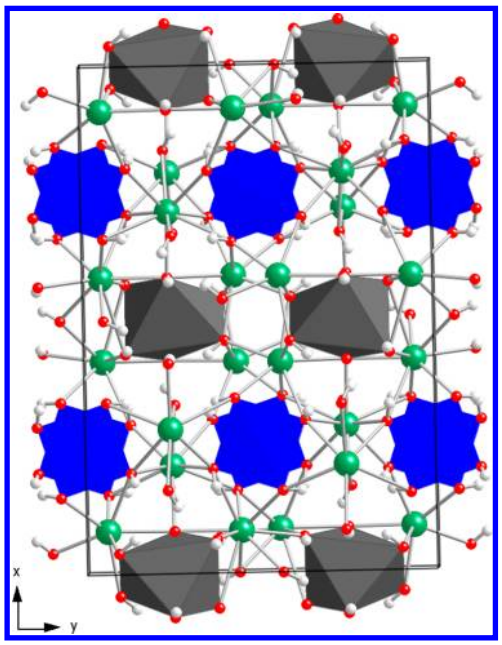

Figure 1. Crystal structure of $Sr_6NaPd_2(OH)_{17}$ (**1**) as viewed down [001]. Sr atoms are shown as green spheres, $Na(OH)_6$ octahedra are dark gray, $Pd(OH)_4$ square planes are blue, O atoms are red spheres, and H atoms are gray spheres.

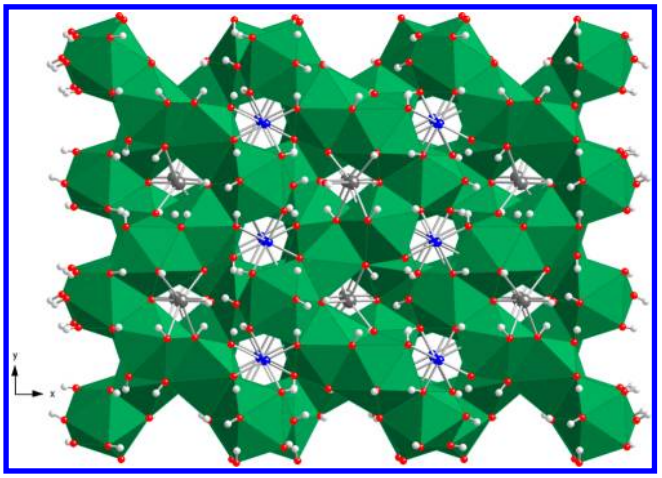

Figure 2. Three-dimensional framework in $Sr_6NaPd_2(OH)_{17}$ (**1**), as viewed down [001]. $Sr(OH)_n$ polyhedra are shown in green, Na atoms are black spheres, Pd atoms are blue spheres, O atoms are red spheres, and H atoms are gray spheres.

two Sr(3) polyhedra, edge shares with four Sr(2) polyhedra, and face shares with one Sr(3) polyhedra. Each Sr(3) polyhedron in the framework shares two corners each with Sr(1) and Sr(2) polyhedra as well as one face each with Sr(1) and Sr(2) polyhedra and two faces with Sr(3) polyhedra. $Pd(OH)_4$ square planes in the channels edge and corner share with Sr(1), Sr(2), and Sr(3) polyhedra. $Na(OH)_6$ octahedra share corners with all three Sr polyhedra but share faces only with Sr(1) and Sr(2) polyhedra.

Although a binary palladium hydroxide $(Pd(OH)_2)$[6] is known, little work has been done on complex palladium hydroxide systems. In fact, the only reports of higher order palladium hydroxides are $K_2Pd(OH)_4$,[10] $A_2Pd(OH)_6$ (A = Na, K),[8] $APd(OH)_4$ (*A* = Ca, Sr, Ba),[9,11] $CaPd(OH)_6$,[7] and $Sr_4Pd(OH)_{10}$.[11] $A_2Pd(OH)_6$ and $CaPd(OH)_6$ phases are rare examples of solid-state compounds containing octahedral Pd^{4+} in the form of $Pd(OH)_6^{2-}$ anions. It should be noted that these three compounds were structurally identified only by comparison of their X-ray powder diffraction patterns to those of their Pt analogs. Therefore, it would be worthwhile to further investigate the structures of these compounds by single-crystal X-ray diffraction.

The remaining examples of complex palladium hydroxides, including the current example of $Sr_6NaPd_2(OH)_{17}$ (**1**), all feature square planar Pd^{2+} in the form of $Pd(OH)_4^{2-}$ anions. $K_2Pd(OH)_4$ and $BaPd(OH)_4$ were solved by single-crystal X-ray diffraction. Subsequently, it was determined for the Ba compound that the structure also contained coordinated water molecules, for a formula of $BaPd(OH)_4{\cdot}H_2O$. Unit cell parameters of $SrPd(OH)_4$ were reported on the basis of indexing powder X-ray diffraction data. Compositions of $CaPd(OH)_4$ and $Sr_4Pd(OH)_{10}$ were determined only by elemental analysis; bonding environments of Pd were inferred from IR spectroscopic data.

$Li_2Pt(OH)_6$ (**2**) and $Na_2Pt(OH)_6$ (**3**) crystallize in space group *P*-3 of the trigonal system (Figure 3). Previously,

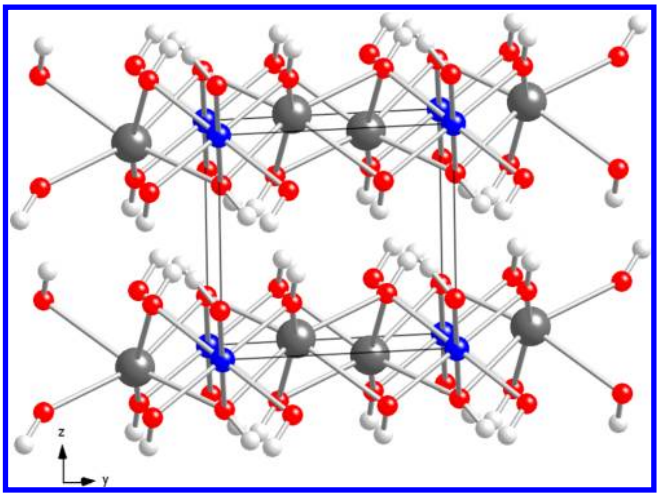

Figure 3. Crystal structure of $A_2Pt(OH)_6$ (A = Li (**2**), Na (**3**)), as viewed down [100]. A atoms are shown as black spheres, Pt atoms are blue spheres, O atoms are red spheres, and H atoms are gray spheres.

structures for these compounds had been reported in space group *P*-31*m* on the basis of powder X-ray diffraction data.[13,15] Initial refinement of our single-crystal X-ray diffraction data in space group *P*-31*m* led to an abnormally large displacement parameter for the alkali metal site. Subsequent refinement in the lower symmetry space group *P*-3 converged rapidly to a satisfactory solution with no unusual displacement parameters.

The asymmetric unit for $A_2Pt(OH)_6$ (*A* = Li (**2**), Na (**3**)) contains one unique crystallographic site for each of the atoms A, Pt, O, and H. The A atom has site symmetry 3.., the Pt atom has site symmetry −3.., and the O and H atoms are on general positions. The Pt atoms are coordinated by a regular octahedron of OH^- anions. The A atoms are bonded to 6 OH^- anions with a distorted octahedral geometry. In order to preserve charge balance, the formal oxidation state of Pt must be +4.

Compounds $A_2Pt(OH)_6$ (**2** and **3**) possess a layered structure, with infinite two-dimensional sheets of $A(OH)_6$ and $Pt(OH)_6$ polyhedra (Figure 4). Each $Pt(OH)_6$ octahedron shares 6 edges with neighboring $A(OH)_6$ octahedra and is

dx.doi.org/10.1021/ic302439b | *Inorg. Chem.* XXXX, XXX, XXX−XXX

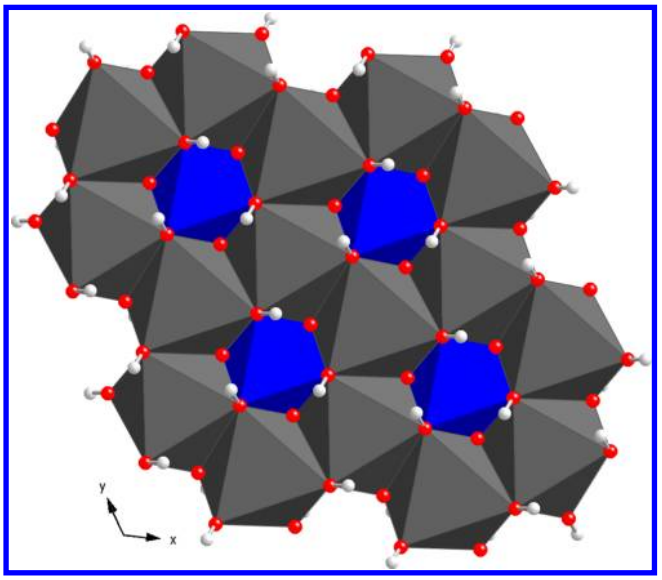

Figure 4. Two-dimensional layer in $A_2Pt(OH)_6$ (A = Li (**2**), Na (**3**)), as viewed down [001]. $A(OH)_6$ octahedra are shown in dark gray, $Pt(OH)_6$ octahedra are shown in blue, O atoms are red spheres, and H atoms are gray spheres.

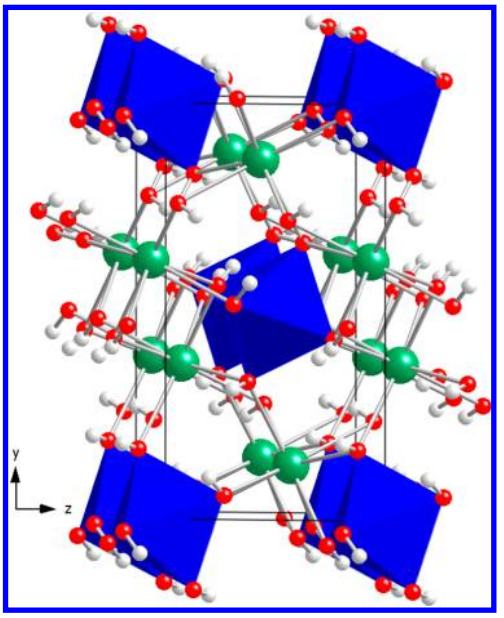

Figure 5. Crystal structure of $Sr_2Pt(OH)_8$ (**4**), as viewed down [100]. Sr atoms are shown as green spheres, $Pt(OH)_6$ octahedra are blue, O atoms are red spheres, and H atoms are gray spheres.

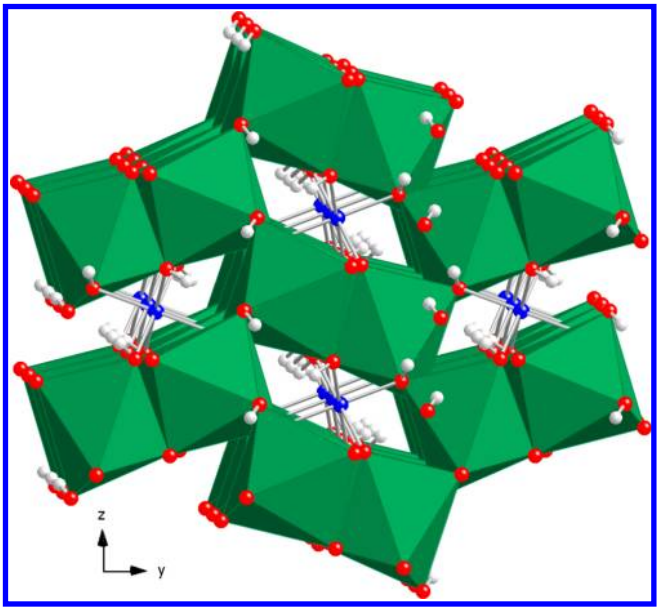

Figure 6. Three-dimensional framework in $Sr_2Pt(OH)_8$ (**4**), as viewed down [100]. $Sr(OH)_8$ dodecahedra are shown in green, Pt atoms are blue spheres, O atoms are red spheres, and H atoms are gray spheres.

completely isolated from neighboring $Pt(OH)_6$ octahedra. Every $A(OH)_6$ octahedron shares 3 edges each with adjacent $A(OH)_6$ and $Pt(OH)_6$ octahedra. Hydroxyl groups point toward the interlayer spaces, and neighboring sheets are presumably held together by hydrogen bonding.

Similar to the case of Pd, the binary hydroxides of Pt ($Pt(OH)_2$ and $Pt(OH)_4$)[12] are known but there has been minimal investigation of more complex platinum hydroxides. The structure of the parent phase platinic acid, H_8PtO_6 (also referred to as $PtO_2{\cdot}4H_2O$, $Pt(OH)_4{\cdot}2H_2O$, or $H_2Pt(OH)_6$), was solved by single-crystal X-ray diffraction.[17] Replacing free protons by other monovalent cations resulted in the following compounds: $(NH_4)_2Pt(OH)_6$,[18] $Li_2Pt(OH)_6$,[13,15] $Na_2Pt(OH)_6$,[13,15] and $K_2Pt(OH)_6$.[20] Only the structure of $K_2Pt(OH)_6$ was solved on the basis of single-crystal X-ray diffraction data. Other structures were indexed via powder X-ray diffraction, and as noted above, space group assignments for $Li_2Pt(OH)_6$ and $Na_2Pt(OH)_6$ appear incorrect. One common feature of all these compounds is that they contain Pt^{4+} in the form of octahedral $Pt(OH)_6^{2-}$ anions.

$Sr_2Pt(OH)_8$ (**4**) crystallizes in space group $P2_1/c$ of the monoclinic system (Figure 5) and is isostructural to $Sr_2Sn(OH)_8$.[39] The asymmetric unit is comprised of one Sr atom, one Pt atom, four O atoms, and four H atoms. The Pt atom is located on an inversion center; all other atoms are located on general positions. The Pt atom is coordinated with a regular octahedron of OH^- anions. The Sr atom is bonded to 8 OH^- anions with a dodecahdedral (bisdisphenoidal) geometry. To achieve charge electroneutrality, a formal oxidation state of +4 is assigned to Pt.

The structure of $Sr_2Pt(OH)_8$ (**4**) is composed of a three-dimensional framework of the $Sr(OH)_8$ dodecahedra, with $Pt(OH)_6$ octahedra occupying the voids (Figure 6). In the framework, each $Sr(OH)_8$ dodecahedron shares 2 corners with $Pt(OH)_6$ octahedra, 2 edges with $Pt(OH)_6$ octahedra, and 4 edges with $Sr(OH)_8$ dodecahedra. Every $Pt(OH)_6$ octahedron shares 4 corners and 4 edges with neighboring $Sr(OH)_8$ dodecahedra.

$Ba_2Pt(OH)_8$ (**5**) crystallizes in a new structure type in space group *Pbca* of the orthorhombic system (Figure 7). The asymmetric unit contains one Ba atom, one Pt atom, four O atoms, and four H atoms. The Pt atom is located on an inversion center, while all other atoms are on general positions. The Pt atom has a regular octahedral coordination of OH^- anions. The Ba atom is bonded to 9 OH^- anions in an irregular square face tricapped trigonal prismatic geometry. As in previous compounds, the formal oxidation state of Pt is once again +4.

The structure of $Ba_2Pt(OH)_8$ (**5**) is three-dimensional with sheets of $Ba(OH)_9$ polyhedra separated by $Pt(OH)_6$ octahedra (Figure 8). Each $Ba(OH)_9$ polyhedron shares 1 corner and 3

dx.doi.org/10.1021/ic302439b | *Inorg. Chem.* XXXX, XXX, XXX–XXX

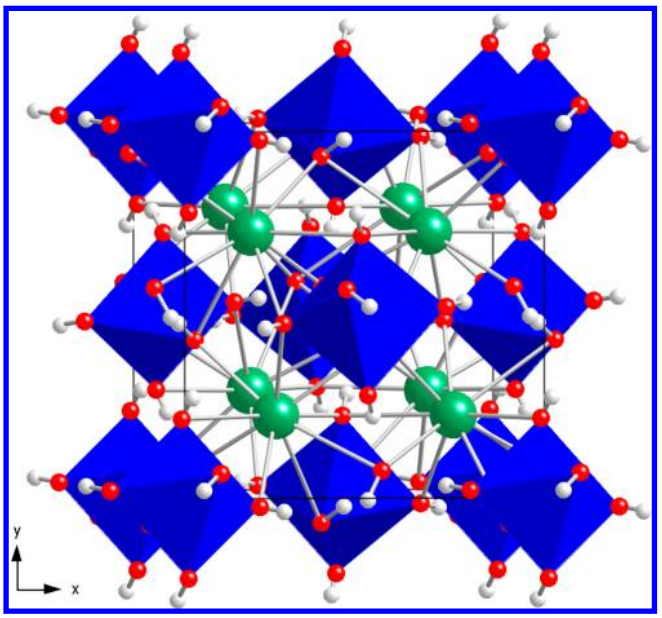

Figure 7. Crystal structure of $Ba_2Pt(OH)_8$ (**5**), as viewed down [001]. Ba atoms are shown as green spheres, $Pt(OH)_6$ octahedra are blue, O atoms are red spheres, and H atoms are gray spheres.

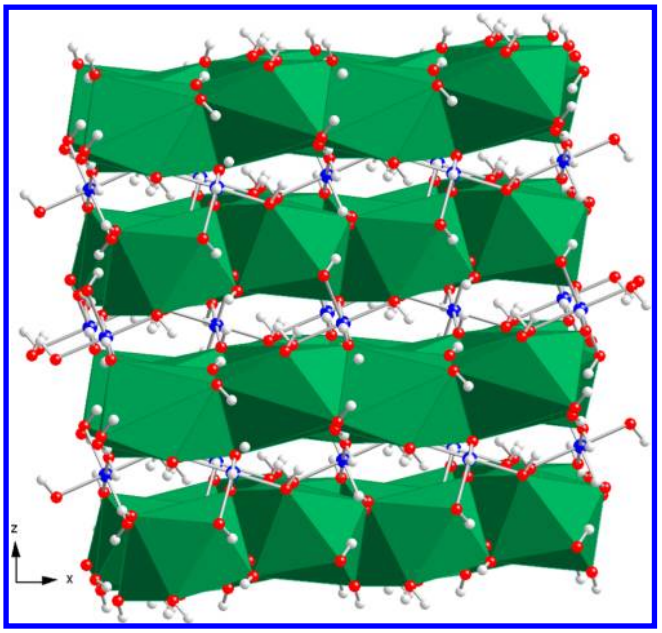

Figure 8. Three-dimensional stacking of layers in $Ba_2Pt(OH)_8$ (**5**), as viewed down [010]. $Ba(OH)_9$ polyhedra are shown in green, Pt atoms are blue spheres, O atoms are red spheres, and H atoms are gray spheres.

edges with neighboring $Pt(OH)_6$ octahedra. Additionally, within the sheet, every $Ba(OH)_9$ polyhedron shares 2 edges, corners, and faces with adjacent $Ba(OH)_9$ polyhedra. Every $Pt(OH)_6$ octahedron shares 2 corners and 6 edges with $Ba(OH)_9$ polyhedra but is completely isolated from other $Pt(OH)_6$ octahedra.

The only previously reported examples of alkaline earth metal platinum hydroxides are $CaPt(OH)_6$,[14] $CaPtO_2(OH)_2$,[16] $SrPt(OH)_6{\cdot}2H_2O$,[16] $BaPt(OH)_6$,[16] and $BaPt(OH)_6{\cdot}H_2O$.[19] The structure of $CaPt(OH)_6$ was reported on the basis of indexing powder X-ray diffraction data, whereas that of $BaPt(OH)_6{\cdot}H_2O$ was determined from refinement of single-crystal X-ray diffraction data. The three remaining compositions were identified only by elemental analysis with no structural data. Similar to their alkali metal containing counterparts as well as the current compounds, all of these phases contain Pt^{4+} in the form of octahedral $Pt(OH)_6^{2-}$ anions.

It is interesting to note here that unlike the previously reported series $A_2M(OH)_6$ (A = Sr, Ba; M = Mn, Co, Ni, Cu),[5] $Sr_2Pt(OH)_8$ (**4**) and $Ba_2Pt(OH)_8$ (**5**) are not isostructural. Perhaps due to steric reasons, the larger Ba^{2+} cation (ionic radius of 1.42 Å)[40] cannot fit into the 8-coordinate site occupied by the smaller Sr^{2+} cation (ionic radius of 1.26 Å)[40] in $Sr_2Pt(OH)_8$ (**4**). This results in the change in structure type and allows Ba^{2+} to fit more comfortably in the 9-coordinate site of $Ba_2Pt(OH)_8$ (**5**).

Thermal Decomposition. The experimental powder X-ray diffraction pattern of the $Na_2Pt(OH)_6$ (**3**) sample was in agreement with the simulated powder X-ray diffraction pattern from the single-crystal X-ray structure determination (Figure 9). This confirmed the phase purity of the sample prior to thermal analysis. Thermal analysis of $Na_2Pt(OH)_6$ (**3**) in air up to a temperature of 1000 °C showed several weight loss steps corresponding to a total weight loss of approximately 16.5% (Figure 10). The following is the proposed decomposition process for $Na_2Pt(OH)_6$ (**3**) in air

$$Na_2Pt(OH)_6 \rightarrow \alpha\text{-}Na_2PtO_3 + 3H_2O$$

The experimentally measured final mass, 17.6630 mg, corresponds very well with the calculated final mass (17.6973 mg) for this proposed decomposition process. Powder X-ray diffraction of the final product confirmed the identity of the material as α-Na_2PtO_3 (Figure 9).[41] Previously, α-Na_2PtO_3 had been made via two routes: (1) starting with a 1:1 ratio of Na_2CO_3 and Pt, heated in O_2 at 700−750 °C,[42] and (2) starting with a 1.3:1 ratio of Na_2O_2 and Pt, heated in O_2 at 900 °C for 1 h.[41] Due to the known volatility of alkali metal oxides at high temperatures, an excess of Na_2O_2 in the second route is necessary to prevent any trace impurity of unreacted Pt metal, as found in the first route. A pure, dark yellow powder was obtained from the second route, from which the material was structurally characterized and determined to belong to the Li_2SnO_3 structure type.[43]

The experimental powder X-ray diffraction pattern of the $Li_2Pt(OH)_6$ (**2**) sample revealed the presence of metallic Pt as an impurity. This mixture was heated in air in a furnace at 1000 °C for 6 h, followed by cooling to room temperature. Powder X-ray diffraction of the final product identified the material as Li_2PtO_3 (as well as metallic Pt). Synthesis of Li_2PtO_3 had previously been reported using Li_2CO_3 and Pt as starting reagents.[44,45] Heating these compounds at 800 °C for 1 day yielded Li_2PtO_3 with remaining Pt metal impurities. An improved synthesis was reported whereby the precursors were heated first at 750 °C for 12 h and then at increments of 50 °C up to 1050 °C for 12 h each with intermittent grinding steps.[46] This procedure yielded phase-pure Li_2PtO_3, from which the structure was refined by the Rietveld method applied to powder X-ray diffraction data.

The experimental powder X-ray diffraction pattern of the $Sr_2Pt(OH)_8$ (**4**) sample was in agreement with the simulated powder X-ray diffraction pattern from the single-crystal X-ray structure determination; however, a few peaks remained which could not be indexed. Thermal analysis of $Sr_2Pt(OH)_8$ (**4**) in air up to a temperature of 1000 °C showed several weight loss steps corresponding to a total weight loss of approximately 16%

dx.doi.org/10.1021/ic302439b | Inorg. Chem. XXXX, XXX, XXX−XXX

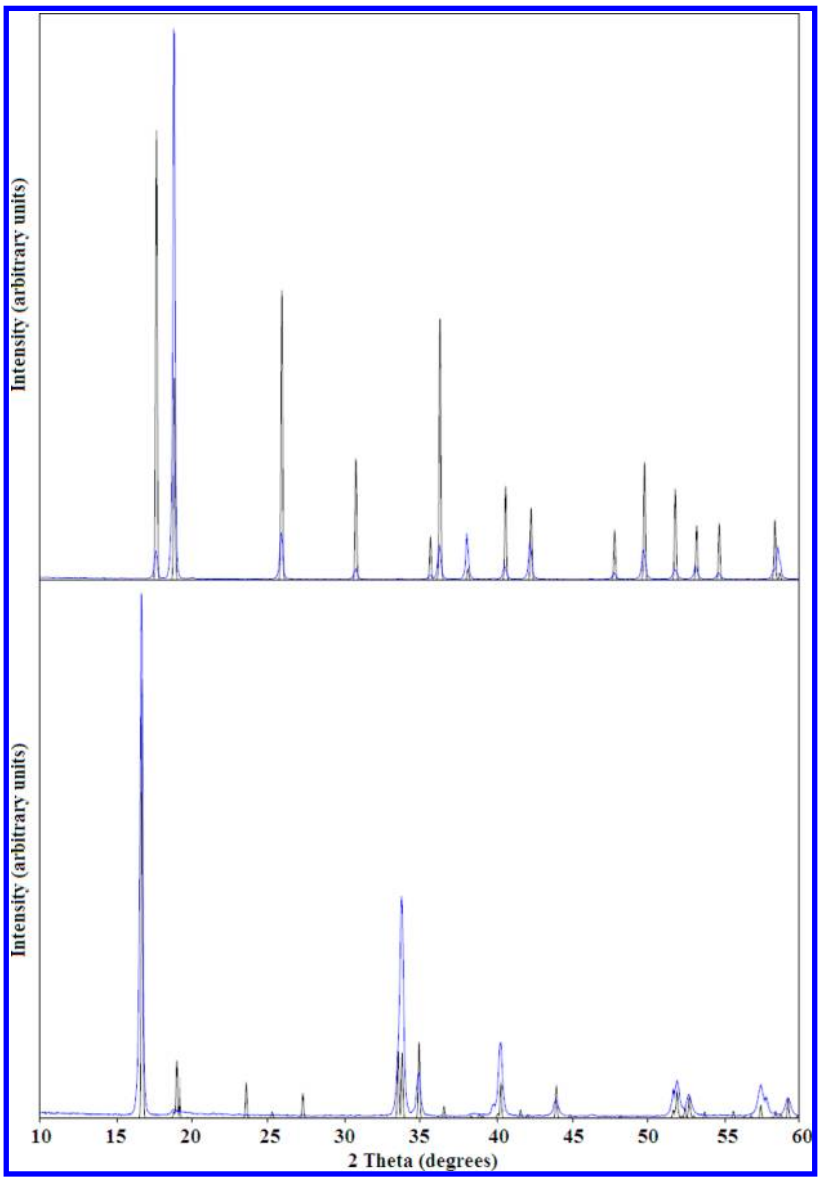

Figure 9. Experimental powder X-ray diffraction patterns for ground single crystals of $Na_2Pt(OH)_6$ (**3**) before (top) and after (bottom) thermogravimetric analysis are shown in blue. Simulated powder X-ray diffraction patterns for $Na_2Pt(OH)_6$ (top) and α-Na_2PtO_3 (bottom) are shown in black.

(Figure 10). For the isostructural compound $Sr_2Sn(OH)_8$,[39] a decomposition process was proposed whereby this compound lost four H_2O molecules in converting first to a mixture of $SrSnO_3$ and $Sr(OH)_2$ between 300 and 700 °C, which reacted further to form Sr_2SnO_4 above 900 °C. The experimentally measured final mass, 16.2107 mg, corresponds somewhat well with the calculated final mass (16.5518 mg) for this proposed decomposition process to a final product of Sr_2PtO_4, which has not been reported in the literature. However, powder X-ray diffraction of the final product instead showed the presence primarily of Sr_4PtO_6[47] and Pt metal. This indicates that a more complicated thermal decomposition process is taking place, perhaps one dependent on the unidentified impurities in the starting sample. The presence of Pt metal in the final product suggests that formation of Sr_4PtO_6 is favored over that of Sr_2PtO_4, resulting in "excess" Pt metal as the ratio of Sr to Pt is increased from 2:1 in the starting material ($Sr_2Pt(OH)_8$ (**4**)) to 4:1 in the final product (Sr_4PtO_6).

CONCLUSION

The hydroflux crystal growth technique has been extended to include platinum group metal containing hydroxides. $Sr_6NaPd_2(OH)_{17}$ (**1**), $Sr_2Pt(OH)_8$ (**4**), and $Ba_2Pt(OH)_8$ (**5**) have been prepared and structurally characterized by single-crystal X-ray diffraction for the first time. Structures of $Li_2Pt(OH)_6$ (**2**) and $Na_2Pt(OH)_6$ (**3**) were reported previously on the basis of powder X-ray diffraction, but the structures have now been corrected via single-crystal X-ray diffraction. Thermal decomposition of these complex metal hydroxides by dehydration and their conversion to metal oxides has been investigated. This method shows potential as a low-temperature alternative to traditional high-temperature syntheses, with the possibility that it may even be able to uncover oxides not attainable by high-temperature solid-state routes.

dx.doi.org/10.1021/ic302439b | *Inorg. Chem.* XXXX, XXX, XXX–XXX

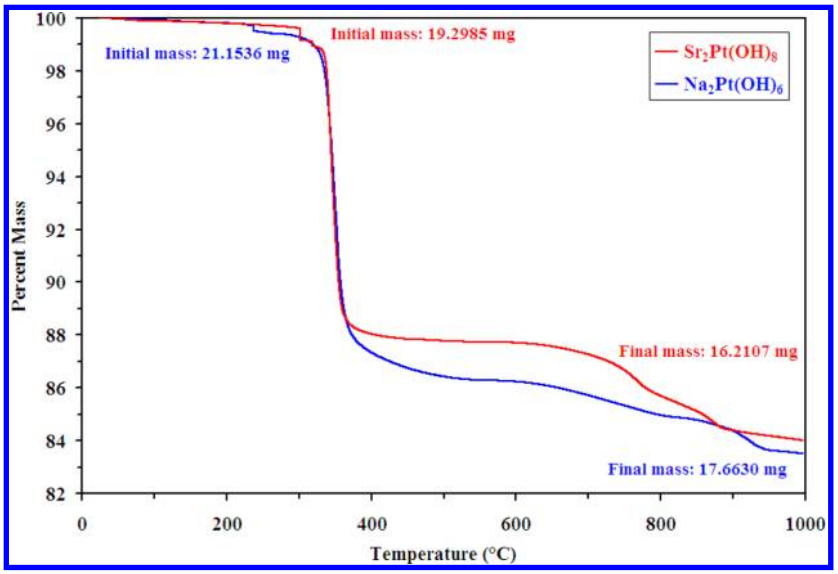

Figure 10. Thermogravimetric analysis data plots for $Na_2Pt(OH)_6$ (**3**, blue) and $Sr_2Pt(OH)_8$ (**4**, red) showing the percent mass as a function of temperature.

■ ASSOCIATED CONTENT

Supporting Information

X-ray crystallographic files in CIF format and IR spectra for $Sr_6NaPd_2(OH)_{17}$ (**1**), $Li_2Pt(OH)_6$ (**2**), $Na_2Pt(OH)_6$ (**3**), $Sr_2Pt(OH)_8$ (**4**), and $Ba_2Pt(OH)_8$ (**5**). This material is available free of charge via the Internet at http://pubs.acs.org.

■ AUTHOR INFORMATION

Corresponding Author

*E-mail: zurloye@mail.chem.sc.edu.

Notes

The authors declare no competing financial interest.

■ ACKNOWLEDGMENTS

This research was supported by the Heterogeneous Functional Materials for Energy Systems (HeteroFoaM) Energy Frontiers Research Center (EFRC), funded by the Department of Energy Office of Basic Energy Sciences under Award Number DE-SC0001061.

■ REFERENCES

(1) Elwell, D.; Scheel, H. J. *Crystal Growth from High-Temperature Solutions*; Academic Press: New York, 1975;
(2) Bugaris, D. E.; zur Loye, H.-C. *Angew. Chem., Int. Ed.* **2012**, *51*, 3780.
(3) Mugavero, S. J., III; Gemmill, W. R.; Roof, I. P.; zur Loye, H.-C. *J. Solid State Chem.* **2009**, *182*, 1950.
(4) Bharathy, M.; Smith, M. D.; zur Loye, H.-C. *Solid State Sci.* **2010**, *12*, 222.
(5) Chance, W. M.; Bugaris, D. E.; zur Loye, H.-C. Unpublished results.
(6) Glemser, O.; Peuschel, G. *Z. Anorg. Allg. Chem.* **1955**, *281*, 44.
(7) Venskovskii, N. U.; Ivanov-Emin, B. N.; Lin'ko, I. V. *Russ. J. Inorg. Chem.* **1983**, *28*, 605.
(8) Venskovskii, N. U.; Ivanov-Emin, B. N.; Lin'ko, I. V. *Koord. Khim.* **1984**, *10*, 1263.
(9) Ivanov-Emin, B. N.; Petrishcheva, L. P.; Zaitsev, B. E.; Ivlieva, V. I.; Izmailovich, A. S.; Dolganev, V. P. *Russ. J. Inorg. Chem.* **1984**, *29*, 1169.
(10) Il'inets, A. M.; Ivanov-Emin, B. N.; Petrishcheva, L. P.; Izmailovich, A. S. *Koord. Khim.* **1987**, *13*, 1660.
(11) Zaitsev, B. E.; Ivanov-Emin, B. N.; Petrishcheva, L. P.; Il'inets, A. M.; Baturin, N. A.; Regel', L. L.; Dolganev, V. P. *Russ. J. Inorg. Chem.* **1991**, *36*, 74.
(12) Wöhler, L.; Martin, F. *Z. Elektrochem. Angew. Phys. Chem.* **1910**, *15*, 791.
(13) Trömel, M.; Lupprich, E. *Naturwissenschaften* **1973**, *60*, 350.
(14) Trömel, M.; Lupprich, E. *Naturwissenschaften* **1973**, *60*, 351.
(15) Trömel, M.; Lupprich, E. *Z. Anorg. Allg. Chem.* **1975**, *414*, 160.
(16) Trömel, M.; Lupprich, E. *Z. Anorg. Allg. Chem.* **1975**, *414*, 169.
(17) Scott, H. G. *Acta Crystallogr., Sect. B: Struct. Sci.* **1979**, *35*, 3014.
(18) Bandel, G.; Platte, C.; Trömel, M. *Z. Anorg. Allg. Chem.* **1981**, *472*, 95.
(19) Bandel, G.; Platte, C.; Trömel, M. *Z. Anorg. Allg. Chem.* **1981**, *477*, 178.
(20) Bandel, G.; Platte, C.; Trömel, M. *Acta Crystallogr., Sect. B: Struct. Sci.* **1982**, *38*, 1544.
(21) Nowogrocki, G.; Abraham, F.; Tréhoux, J.; Thomas, D. *Acta Crystallogr., Sect. B: Struct. Sci.* **1976**, *32*, 2413.
(22) Elout, M. O.; Haije, W. G.; Maaskant, W. J. A. *Inorg. Chem.* **1988**, *27*, 610.
(23) Fischer, D.; Hoppe, R. *Z. Anorg. Allg. Chem.* **1991**, *601*, 41.
(24) Porai-Koshits, M. A.; Atovmyan, L. O.; Andrianov, V. G. *Zh. Strukt. Khim.* **1961**, *2*, 743.
(25) Atovmyan, L. O.; Andrianov, V. G.; Porai-Koshits, M. A. *Zh. Strukt. Khim.* **1962**, *3*, 685.
(26) Nevskii, N. N.; Ivanov-Emin, B. N.; Nevskaya, N. A.; Belov, N. V. *Dokl. Akad. Nauk SSSR* **1982**, *266*, 628.
(27) Nevskii, N. N.; Ivanov-Emin, B. N.; Nevskaya, N. A.; Belov, N. V. *Dokl. Akad. Nauk SSSR* **1982**, *266*, 1138.
(28) Nevskii, N. N.; Porai-Koshits, M. A. *Dokl. Akad. Nauk SSSR* **1983**, *270*, 1392.
(29) Nevskii, N. N.; Porai-Koshits, M. A. *Dokl. Akad. Nauk SSSR* **1983**, *272*, 1123.
(30) Jewiss, H. C.; Levason, W.; Tajik, M.; Webster, M.; Walker, N. P. C. *J. Chem. Soc., Dalton Trans.* **1985**, *1*, 199.
(31) Tomaszewska, A.; Müller-Buschbaum, H. K. *J. Alloys Compd.* **1993**, *194*, 163.
(32) Murmann, R. K.; Barnes, C. L. *Z. Kristallogr.-New Cryst. Struct.* **2002**, *217*, 303.
(33) Mogare, K. M.; Klein, W.; Jansen, M. *Acta Crystallogr., Sect. E: Struct. Rep.* **2006**, *62*, i52.
(34) Zhai, Y.; Pierre, D.; Si, R.; Deng, W.; Ferrin, P.; Nilekar, A. U.; Peng, G.; Herron, J. A.; Bell, D. C.; Saltsburg, H.; Mavrikakis, M.; Flytzani-Stephanopoulos, M. *Science* **2010**, *329*, 1633.

(35) Horwat, D.; Dehmas, M.; Gutiérrez, A.; Pierson, J.-F.; Anders, A.; Soldera, F.; Endrino, J.-L. *Chem. Mater.* **2012**, *24*, 2429.
(36) Rudnick, P.; Cooke, R. D. *J. Am. Chem. Soc.* **1917**, *39*, 633.
(37) *SMART Version 5.625, SAINT+ Version 6.22, and SADABS Version 2008/1*; Bruker Analytical X-Ray Instruments: Madison, WI, 2008;
(38) Sheldrick, G. M. *Acta Crystallogr., Sect. A: Found. Crystallogr.* **2008**, *64*, 112.
(39) Wu, M.; Li, X.; Shen, G.; Li, J.; Xu, R.; Proserpio, D. M. *J. Solid State Chem.* **2000**, *151*, 56.
(40) Shannon, R. D. *Acta Crystallogr., Sect. A: Found. Crystallogr.* **1976**, *32*, 751.
(41) Urland, W.; Hoppe, R. *Z. Anorg. Allg. Chem.* **1972**, *392*, 23.
(42) Scheer, J. J.; van Arkel, A. E.; Heyding, R. D. *Can. J. Chem.* **1955**, *33*, 683.
(43) Lang, G. *Z. Anorg. Allg. Chem.* **1966**, *348*, 246.
(44) Asakura, K.; Okada, S.; Arai, H.; Tobishima, S.-i.; Sakurai, Y. *J. Power Sources* **1999**, *81*−*82*, 388.
(45) Okada, S.; Yamaki, J.-i.; Asakura, K.; Ohtsuka, H.; Arai, H.; Tobishima, S.-i.; Sakurai, Y. *Electrochim. Acta* **1999**, *45*, 329.
(46) O'Malley, M. K.; Verweij, H.; Woodward, P. M. *J. Solid State Chem.* **2008**, *181*, 1803.
(47) Randall, J. J., Jr.; Katz, L. *Acta Crystallogr.* **1959**, *12*, 519.